Determining carrier mobility with a metal–insulator–semiconductor structure

P. Stallinga [a,*], A.R.V. Benvenho [a], E.C.P. Smits [b], S.G.J. Mathijssen [b], M. Cölle [b], H.L. Gomes [a], D.M. de Leeuw [b]

[a] Universidade do Algarve, Center of Electronics, Opto-electronics and Telecommunications, Campus de Gambelas, 8005-139 Faro, Portugal
[b] Philips Research Laboratories, Professor Holstlaan 4, 5656 AA Eindhoven, The Netherlands

ARTICLE INFO

ABSTRACT

The electron and hole mobility of nickel-bis(dithiolene) (NiDT) are determined in a metal–insulator–semiconductor (MIS) structure using admittance spectroscopy. The relaxation times found in the admittance spectra are attributed to the diffusion time of carriers to reach the insulator interface and via Einstein's relation this yields the mobility values. In this way, an electron mobility of 1.9×10^{-4} cm^2/Vs and a hole mobility of 3.9×10^{-6} cm^2/Vs were found. It is argued that the low mobility is caused by an amphoteric mid-gap trap level. The activation energy for electrons and holes from these traps is found to be 0.46 eV and 0.40 eV, respectively.

© 2008 Elsevier B.V. All rights reserved.

1. Introduction

The charge-carrier mobility (henceforth simply called 'mobility', or μ) is an important parameter of semiconductor materials and is the major determining factor for the speed of electronic devices. The mobility is defined as the relation of the drift velocity of the carriers to the electric field, $v = \mu E$ [1]. In semiconductors there are two types of carriers, electrons and holes, and they can have different mobilities, in crystalline materials mostly due to different effective mass (for example, in silicon the electron and hole mobility are about 1500 and 500 cm^2/Vs, respectively). In spite of its simple definition, because of the difficulty of measuring velocity, accurate determination of the mobility of the carriers is not easy and indirect ways are used, each with its own advantages and disadvantages. The most popular are current–voltage, time-of-flight, Hall measurements and field-effect-transistor.

Hall measurements are inadequate for low-mobility materials because of the tiny quantities that then have to be measured. In standard I–V curves, the mobility cannot be measured because, in the ohmic regime, the current depends on the product of charge density *and* mobility. Independent determination of mobility is impossible. This problem can be circumvented by measuring in the so-called space-charge limited current regime, which depends only on mobility [2–4]. However, when the mobility depends on electric field (for instance in the presence of traps, as in Poole–Frenkel conduction) the extraction is more complicated, because across the device the field is not constant and therefore also not a constant mobility is measured [4]. Blom et al., have used the I–V technique in systems with electron traps exponentially distributed in energy. Mobility values could then only be given for the hole-conduction SCLC regime [5].

* Corresponding author.
E-mail address: pjotr@ualg.pt (P. Stallinga).

In time-of-flight measurements, a high electron–hole density is created close to one surface of the sample by a light pulse. One type of carrier is then driven by an electrical field to the other surface. The current transient is monitored, and the characteristic time is a measure for the mobility. In highly disordered materials, the transients get distorted and extraction of the mobility more complicated [6].

A more popular technique, especially for low-mobility materials, is with a (thin-film) field-effect-transistor (TFT). The mobility is directly proportional to the derivative of a so-called transfer curve of drain–source current vs. gate–source bias. However, when traps are present, the transfer curves become highly non-linear and mobility starts being a function of bias and/or temperature, depending on the distributions of traps and conductive states [7]. In view of this, it is not clear how to define a way that will result in a unique mobility value.

Here we present a way to determine the mobility in an alternative way by means of a metal–insulator–semiconductor (MIS) diode structure. The method resembles time-of-flight, but the measurements are not done in the time domain, but in the frequency domain. Instead of measuring current transients, impedance/admittance spectra are acquired. The advantage of using MIS structures above regular diodes is that they do not have DC conductance which otherwise might mask the relevant admittance data. As a comparison, Martens et al., have endeavored to determine the electron and hole mobility by a similar technique, but instead in an LED structure [8,9], later again studied by Tsang et al. [10] (and even more recently by Schmeits [11] and an elaborate example by Nguyen et al. [12]). These devices need dual injection of carriers, i.e., both electrons and holes simultaneously. The analysis becomes thus complicated and leaves room for doubt, see for example their different correction factors (0.29 and 0.56, respectively) to convert the relaxation time of admittance spectroscopy to time-of-flight and thus mobility. In contrast, the MIS structure can easily be put in a one-carrier-type state (either holes or electrons) and this facilitates the analysis, as will be shown here.

2. Experimental

Fig. 1 shows a schematic picture of an MIS device used in this work. It consists of a "metal" for which we used, for technological reasons, a highly doped n$^+$-silicon single crystal. For the insulating layer, silicon oxide of thickness $d_{ox} = 200$ nm, thermally grown on the silicon substrate, with a relative permittivity (dielectric constant) of $\varepsilon_{ox} = 3.9$ [1], was used. The semiconductor used is a member of the family of organic materials nickel-bis(dithiolene) (NiDT), see Fig. 1 (R = NMe$_2$), which show ambipolar charge transport and, because of the planar nature of the molecules, can have a relatively high mobility (measured by the field-effect in a TFT) [13–15], though also low mobilities have been reported, especially when exposed to air [16]. The layer was deposited by spin-coating, with thickness d_s=50 nm. According to literature, this material has electron and hole mobility of $\mu_n = 2.0 \times 10^{-5}$ and
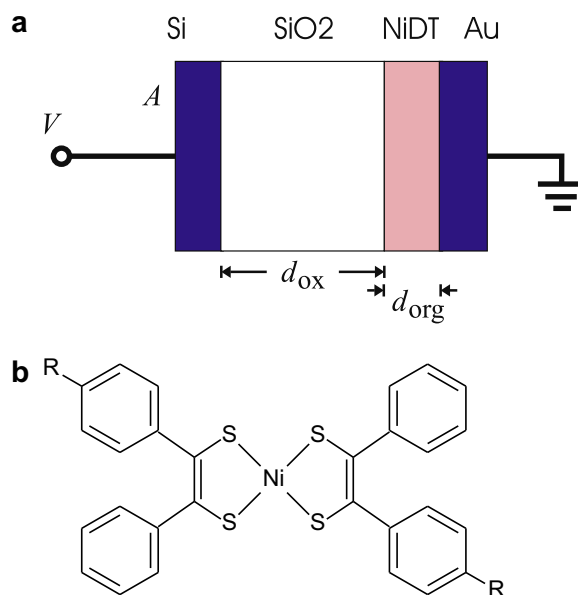

Fig. 1. Left: Schematic cross section of the MIS device consisting of (left to right): a silicon ("metal") electrode, a silicon-oxide insulating layer ($d_{ox} = 200$ nm), NiDT organic semiconductor ($d_s = 50$ nm), and gold electrode (A). The external bias V is applied to the silicon substrate relative to the gold electrode. Right: Nickel-bis(dithiolene) family. For the current work, the member used has R = NMe$_2$.

$\mu_p = 2.5 \times 10^{-4}$ (cm^2/Vs), respectively, as derived from the field-effect in FETs [15]. On top of the organic layer, a gold electrode (typical area $A = 1.3 \times 10^{-5}$ m^2) was deposited by shadow mask. The oxide capacitance is thus typically $C_{ox} = \varepsilon_{ox}\varepsilon_0 A/d_{ox} = 2.2$ nF, where ε_0 is the permittivity of vacuum, and the semiconductor layer capacitance equals $C_s = \varepsilon_{org}\varepsilon_0 A/d_s = 17.4$ nF, where a value for the relative dielectric constant of $\varepsilon_s = 5$ was used for NiDT; a typical value for organic materials. The combined geometric capacitance is thus $C_{geo} = (C_s^{-1} + C_{ox}^{-1})^{-1} = 2.0$ nF. The difference between the maximum and minimum attainable capacitance is thus of the order of 200 pF.

The nickel-bis(dithiolene) was obtained from Sensient GmbH (Germany) and has an energy gap of $E_g = 0.9$ eV, an ionization potential of $I_p = E_{vac} - E_{HOMO} = 5.2$ eV, and an electron affinity of $\chi = E_{vac} - E_{LUMO} = 4.3$ eV, where Koopmans' theorem was used linking the energies and levels [17], and E means energy and the subscripts "vac", "HOMO" and "LUMO" denote vacuum, highest-occupied-molecular-orbit (equivalent to valence band) and lowest-unoccupied-molecular-orbit (equivalent to conduction band), respectively. Considering the high resistivity of the material and the low mobility, we expect deep traps to be present that pin the Fermi level (E_F) somewhere halfway the forbidden gap. Gold has a work function of 5.1 eV [1]. The energy gap of silicon is 1.12 eV at room temperature and its Fermi level is estimated to lie 100 meV below the conduction band, which, in turn is situated 4.05 eV below the vacuum level, $\chi = E_{vac} - E_C$. With these values we are able to reconstruct the band diagram which is schematically shown in Fig. 2. The resistivity of the oxide is much higher than that of the organic layer so that nearly all the
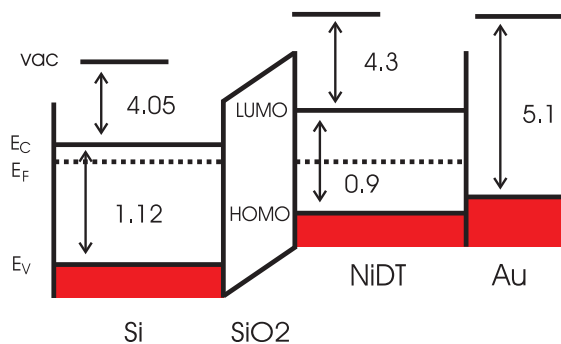
Fig. 2. Schematic band diagram of the device shown in Fig. 1. Values in eV.
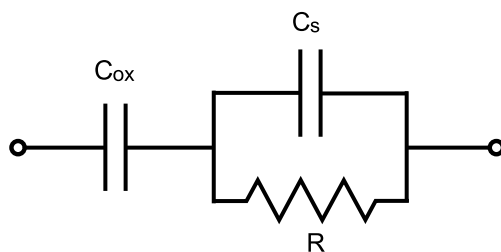

Fig. 3. Equivalent circuit used to simulate the electrical frequency behavior. For low frequencies the capacitance is equal to the oxide capacitance C_{ox}, while for high frequencies the capacitance is equal to the serial sum of C_{ox} and C_s. R does not represent the DC resistance of the organic layer but is merely a parameter that describes the frequency behavior, according to Eq. (3).

built-in voltage and applied external biases are absorbed by the oxide. It is assumed that gold is forming an ohmic contact with the organic material. For this reason we have omitted a Schottky barrier at this end of the device in the figure, although on basis of the numbers given above there should be a tiny one (of approx. 0.1 eV and built-in voltage of 0.35 V).

Electrical measurements were performed on a Keithley 487 Picoammmeter (I–V curves) and a Fluke PM 6306 RCL Bridge (impedance spectroscopy). Measurements were performed in low-vacuum (10^{-3} mbar) in a metal cryostat. All measurements were performed at room temperature ($T = 300$ K), unless otherwise specified. Positive bias signifies that the silicon electrode has a higher potential with respect to the gold counter-electrode.

3. Theory

When the organic layer is conductive by accumulation of holes or electrons, the capacitance is equal to the oxide capacitance C_{ox}. However, for the capacitance to have this value, the charges must have enough time to arrive at this interface. For high AC probing frequencies, the charges cannot follow the field oscillations. The time it takes for the charges to reach the interface is given by diffusion, for instance (for holes)

$$\tau = \frac{d_s^2}{D_p} = \frac{q}{kT}\frac{d_s^2}{\mu_p} \tag{1}$$

with D_p the hole diffusion coefficient, q the elementary charge, μ_p the hole mobility and k Boltzmann constant. Here Einstein's relation [18] was used that couples the diffusion coefficient and the mobility, $D_p = \mu_p kT/q$. A similar equation exists for electrons. Eq. (1) defines a cut-off frequency

$$f_c = \frac{1}{2\pi\tau} = \frac{\mu_p kT}{2\pi q d_s^2} \tag{2}$$

For AC-probing frequencies well below this cut-off frequency, the measured capacitance is equal to the oxide capacitance C_{ox}, while far above it, the charges do not enter the organic layer and the capacitance settles at the geometric capacitance value C_{geo}. This can also be electrically modeled by an equivalent circuit consisting of a

capacitance and a resistance in series with a second capacitance, as shown in Fig. 3. The resistance R of the circuit does not represent the DC resistance of the organic layer, but merely models the frequency behavior, with

$$\tau = R(C_{ox} + C_s) \tag{3}$$

At the frequency of Eq. (2), where the capacitance drops, the loss (defined as $L = G/\omega$, with G the conductance and $\omega = 2\pi f$ the angular frequency) has a maximum. In summary, the spectrum of loss has a maximum at a frequency where simultaneously the capacitance drops. This frequency is a direct measure for the diffusion coefficient – and thus the mobility – if the device dimensions are known, see Eq. (2).

4. Results and discussion

For strong-bias, the organic layer is filled with electrons or holes and the resistivity of the organic layer is much lower than that of the insulator. The applied bias is mainly absorbed by the insulating layer and the voltage drop and electric field in the organic material are negligible. Fig. 4 shows a characteristic C–V plot which demonstrates how, under strong-bias, the capacitance at low frequencies is equal to the oxide capacitance C_{ox}. For positive bias the organic layer is full of electrons and this we call 'accumulation of electrons', whereas for strong negative bias holes are pulled into the organic layer and there exists 'accumulation of holes'. For small biases, the device is depleted, the organic layer neither has holes nor electrons and the capacitance reaches a minimum equal to C_{geo}. It is interesting to compare the device to a standard (doped) MIS device. A standard MIS goes from accumulation to inversion. The transition is abrupt when going to inversion, but stretched when going into accumulation and an asymmetric peak results [1]. Our undoped device, ideally, should go abruptly from accumulation of holes to accumulation of electrons and the dip in the C–V plot should be very narrow. The C–V plot of Fig. 4 is indeed symmetric, but the switch from accumulation of holes to accumulation of electrons is not instantaneous. This might be due to a presence of amphoteric deep levels. They can be charged either positively or negatively, thereby contributing to space charge and allowing for band bendings and stretching of the transition. More important, most of the applied
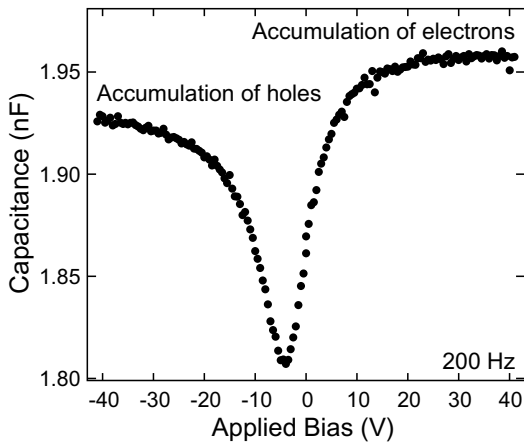
Fig. 4. C–V plot (measured at a frequency of 200 Hz) showing the capacitance is equal to the oxide capacitance C_{ox} for accumulation of holes or electrons. In between there is a bias where the capacitance reaches a minimum equal to the geometric capacitance C_{geo}.

bias is absorbed by the oxide layer and large voltages must be applied in order to cause any changes in the semiconductor layer. This further broadens the dip.

The minimum capacitance of Fig. 4 corresponds to the geometric capacitor formed by the silicon and gold electrodes 'filled' with the oxide and organic layers, as described in the experimental section. It happens for a bias of around −5 V, showing that at 0 V the organic layer is not completely devoid of free electrons.

As described in the theoretical section, the capacitance can be equal to the oxide capacitance C_{ox} *only* if the probing frequency is low enough. Otherwise the measured capacitance is the geometric capacitance C_{geo}. Fig. 5 shows an example of a spectrum of a device. The figure also shows a simulation of the spectrum based on the equivalent circuit given in Fig. 3. Apart from the high-frequency
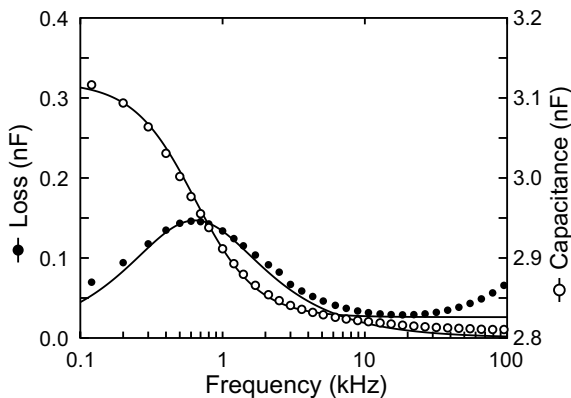
dispersion which we attribute to cables and other instrumental artifacts, the fit is quite well and we can see how the capacitance drops from C_{ox} to C_{geo} at a frequency where the loss has a maximum. From this frequency we can determine the (hole) mobility. The spectrum of Fig. 5 has a maximum at 640 Hz ($\tau = 250\ \mu s$). Eq. (1) with $d_s = 50\ nm$ then gives a hole diffusion coefficient $D_p = 1.0 \times 10^{-11}\ m^2/s$, which translates via Einstein's relation into a hole mobility of $\mu_p = 3.9 \times 10^{-6}\ cm^2/Vs$.

Fig. 6 shows the position of the maximum of the loss as a function of bias. At strong negative bias the frequency is constant and this gives the hole mobility as discussed above. In the same way, for strong positive bias the electron mobility can be determined. The frequency of the maximum in loss is here 31.8 kHz ($\tau = 5\ \mu s$) and this yields an electron mobility of $D_n = 5 \times 10^{-10}\ m^2/s$ $\mu_n = 1.9 \times 10^{-4}\ cm^2/Vs$.

The mobility is rather low and this hints at a huge abundance of deep localized states, also known as traps. When a large density of traps exists, charges spend most of their time on these localized states. To contribute to current they have to be promoted to the appropriate band. The effective mobility is then a weighed average of the trap mobility μ_T and band mobility μ_0. In other words, assuming the trap mobility is zero, the effective mobility is determined by the fraction of the time (α) a charge spends in the bands, $\mu = \alpha\mu_0$. This fraction depends on the temperature and this allows for the determination of the trap depth. Assuming the trap to be discrete and the mobility of charges residing there to be zero and a Boltzmann distribution over the levels, the activation energy of mobility is equal to the trap depth [7]. Since the frequency of the maximum in loss scales linearly with mobility (Eq. (2)), this is equal to the activation energy of this frequency.

Fig. 7 shows an Arrhenius plot of frequency of the maximum of loss as a function of temperature. From the slope we determine that the mobility of holes has an activation energy of $E_{Ap} = 400\ meV$ and the mobility of electrons an

Fig. 5. Example of a spectrum of loss (●) and capacitance (○) at a bias of $V = -28$ V. For low frequencies the charges have enough time during an AC cycle to reach the interface and the measured capacitance is equal to C_{ox}, while for high frequencies the capacitance is the geometric capacitance C_{geo}, *i.e.*, charges do not move into the organic layer. The turning frequency is given by Eq. (2). At this frequency the loss has a maximum. The solid lines are simulations with $C_{ox} = 3.1$ nF, $C_s = 30$ nF and $R = 7.5$ kΩ.
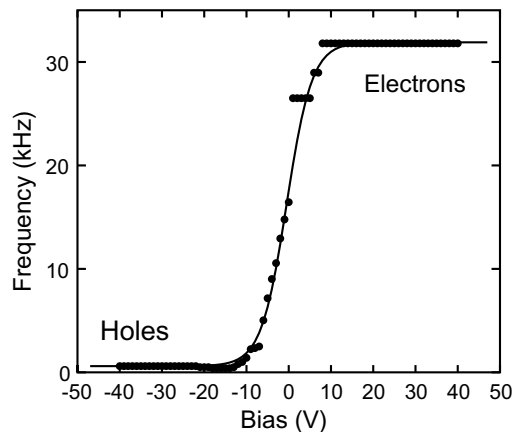

Fig. 6. Frequency of maximum of loss as a function of bias as shown in Fig. 5. The solid line is a guide to the eye. At strong positive or negative bias, the frequency is stable and this allows for the determination of the mobility via Eq. (2).
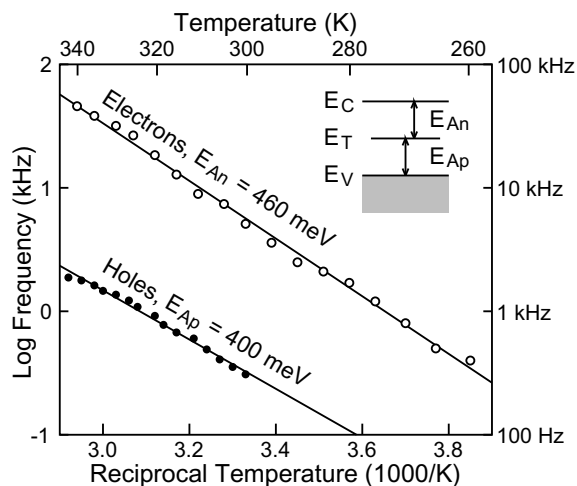
Fig. 7. Arrhenius plot of the frequency of loss as a function of temperature revealing the activation energies of mobility as indicated. The inset shows the energetic position of the responsible traps.

activation energy of $E_{An} = 460$ meV. Considering the fact that the band gap of NiDT is approximately 0.9 eV, this places the responsible traps close to mid-gap, see the energy diagram in the figure. This is in-line with the observation of an amphoteric trap mentioned earlier.

To summarize the experimental results, we have shown here how admittance spectroscopy is used to determine both the electron and hole mobilities in the same NiDT device. Compared to literature, the found mobilities are much lower. Moreover, we find the electron mobility higher than the hole mobility while it has been reported reverse [15]. The reason for this is unknown. However, it is very common that mobilities measured with different techniques result in widely different values.

What is actually measured by this technique is not the mobility, but the diffusion coefficient. They are linked by Einstein's Relation, which has its limitations. As an example, it is valid only when multiple occupancy of the electronic levels is allowed, with uncorrelated particles, like in band conduction. When the particle movements are correlated, the Einstein Relation is no longer valid and diffusion is more rapid than predicted by Einstein's Relation [19]. Another reason can be that Einstein's Relation is violated in non-equilibrium systems [20].

The combination of parameters (film thickness and mobility) puts the interesting frequencies in the range of the experimental set-up used. For materials with mobilities in the order found here the presented method is a valuable additional tool in the determination of the carrier mobility. For higher quality materials, such as crystalline silicon, the cut-off frequency falls above the measurement window, while for low-mobility materials or thick devices, the response becomes too slow and the frequency range inconvenient.

An alternative interpretation of the data which we have considered is assigning the spectral peaks to interface states. When the Fermi level is resonant with these states at the interface, the capacitance is increased and a peak in loss is observed at a frequency determined by the energetic distance of these states to the relevant band to which they communicate and with an amplitude proportional to the density of these states. Changing the bias moves the Fermi level at the interface and other interface states are probed. In this way the energetic profile of these states can be mapped [21]. However, the devices reported here do not behave in accordance to these theories and we find the analysis described here more probable.

References

[1] S.M. Sze, Physics of Semiconductor Devices, second ed., Wiley & Sons, New York, 1981.
[2] D. Ma, I.A. Hümmelgen, X. Jing, Z. Hong, L. Wang, X. Zhao, F. Wang, F.E. Karasz, J. Appl. Phys. 87 (2000) 312.
[3] A.R.V. Benvenho, R. Lessmann, I.A. Hümmelgen, R.M.Q. Mello, R.W.C. Li, F.F.C. Bazito, J. Gruber, Mater. Chem. Phys. 95 (2006) 176.
[4] D. Natali, M. Sampietro, J. Appl. Phys. 92 (2002) 5310.
[5] P.W.M. Blom, M.J.M. de Jong, J.J.M. Vleggaar, Appl. Phys. Lett. 68 (1996) 3308.
[6] H. Scher, E.W. Montroll, Phys. Rev. B 12 (1975) 2455.
[7] P. Stallinga, H.L. Gomes, Org. Electron. 7 (2006) 592.
[8] H.C.F. Martens, J.N. Huiberts, P.W.M. Blom, Appl. Phys. Lett. 77 (2000) 1852.
[9] H.C.F. Martens, H.B. Brom, P.W.M. Blom, H.F.M. Schoo, Phys. Status Solidi 218 (2000) 283.
[10] S.W. Tsang, S.K. So, J.B. Xu, J. Appl. Phys. 99 (2006) 013706.
[11] M. Schmeits, J. Appl. Phys. 101 (2007) 084508.
[12] N.D. Nguyen, M. Schmeits, H.P. Loebl, Phys. Rev. B 75 (2007) 075307.
[13] J.-Y. Cho, B. Domercq, S.C. Jones, J. Yu, X. Zhang, Z. An, M. Bishop, S. Barlow, S.R. Marder, B. Kippelen, J. Mater. Chem. 17 (2007) 2642.
[14] T. Anthopoulos, S. Setayesh, E. Smits, M. Cölle, E. Contatore, B. de Boer, P.W.M. Blom, D.M. de Leeuw, Adv. Mater. 18 (2006) 1900.
[15] E. Smits, T.D. Anthopoulos, S. Setayesh, E. van Veenendaal, R. Coehoorn, P.W.M. Blom, B. de Boer, D.M. de Leeuw, Phys. Rev. B 73 (2006) 205316.
[16] T. Taguchi, H. Wada, T. Kambayashi, B. Noda, M. Goto, T. Mori, K. Ishikawa, H. Takezoe, Chem. Phys. Lett. 421 (2006) 395.
[17] P.W. Atkins, Quanta, A Handbook of Concepts, second ed., Oxford University Press, Oxford, 1991.
[18] A. Einstein, Ann. Phys. 17 (1905) 549.
[19] S.E. Guidoni, C.M. Aldao, Eur. J. Phys. 23 (2002) 395.
[20] T. Speck, U. Seifert, Europhys. Lett. 74 (2006) 391.
[21] P. Stallinga, H.L. Gomes, M. Murgia, K. Müllen, Org. Electron. 3 (2002) 43.